Optical pulling force and conveyor belt effect in resonator–waveguide system

Varat Intaraprasonk[1] and Shanhui Fan[2,*]

[1]*Department of Applied Physics, Stanford University, Stanford, California 94305, USA*

[2]*Department of Electrical Engineering, Stanford University, Stanford, California 94305, USA*

**Corresponding author: shanhui@stanford.edu*

Received June 25, 2013; revised July 29, 2013; accepted July 29, 2013;
posted July 30, 2013 (Doc. ID 192906); published August 21, 2013

We present the theoretical condition and actual numerical design that achieves an optical pulling force in resonator–waveguide systems, where the direction of the force on the resonator is in the opposite direction to the input light in the waveguide. We also show that this pulling force can occur in conjunction with the lateral optical equilibrium effect, such that the resonator is maintained at the fixed distance from the waveguide while experiencing the pulling force. © 2013 Optical Society of America

OCIS codes: (230.4555) Coupled resonators; (350.4855) Optical tweezers or optical manipulation.
http://dx.doi.org/10.1364/OL.38.003264

Optical force is of significant interest since it provides the mechanism to couple mechanical motion with optical field. Some of the recent works on this subject are on the somewhat counterintuitive optical pulling force or negative force, where the optical force on an object is in the opposite direction to that of the incident light [1–8]. Optical pulling force can be achieved by different mechanisms. In [2–4], pulling is achieved using optical gradient force, which attracts the object to spatial locations with higher light intensity. Optical scattering force can also provide pulling force if the object can scatter incident light in a mode with low forward momentum to an outgoing mode with higher forward momentum [5–8]. All previous works on optical pulling force, however, use free-space beams. The diffraction of these beams then becomes a major limitation. While [6–8] use nondiffracting Bessel beams to overcome the difficulties associated with diffraction, a Bessel beam contains infinite power and can only be approximately realized.

A natural way to overcome the diffraction problem is to use a waveguide. Therefore, in this Letter, we design structures that achieve optical pulling force in an on-chip waveguide–resonator system (Fig. 1), where light is incident through a waveguide, and the object experiencing the force is a side-coupled resonator. Various optical force effects related to resonance have been extensively studied before [9,10]. Our focus here is specific to the study of pushing and pulling forces related to the resonance. For this waveguide–resonator system, the lateral force perpendicular to the waveguide has been studied extensively. It has been shown that both repulsive and attractive lateral force can be achieved at resonances [11–18]. The longitudinal force parallel to the waveguide was studied in [17,18] which, however, only reported a pushing force. In this Letter, we show that one can achieve a pulling force in the waveguide–resonator system. We also show that this optical pulling force can be combined with the lateral optical equilibrium effect reported in [16], to achieve an all-optical conveyor belt effect where the object is maintained at the fixed distance from the waveguide while being pulled along the waveguide entirely with optical force.

We start by illustrating the general idea for creating optical pulling force in waveguide–resonator system. As a simple example, we consider a two-mode waveguide. In this Letter, we normalize the parameters to the length scale of a, such that if a is chosen to be 1 μm, the operating free-space wavelength is approximately 1550 nm, which is the telecommunication wavelength. We choose our waveguide to be $0.4a$ wide, made with silicon with permittivity $\epsilon_{\mathrm{Si}} = 12.1$, and surrounded by air with permittivity $\epsilon_{\mathrm{air}} = 1$. We calculate the modes in TM polarization (electric field along the z direction) using a finite-element frequency domain method [19], which is suitable for the simulation of the field excitation of a resonator because an adaptive computational meshing can be easily implemented (we use a grid size of 1/100 to 1/40 of the free-space wavelength in the resonator and the waveguide region, and three-time coarser size for the air region). Note that a coarser grid size is sufficient to calculate the wave propagation inside each region, but the fine grid size is used to accurately describe the curved boundary of the resonator. We found that the computation boundary can be terminated with either a perfectly matched layer or an absorbing boundary condition with little difference.

This waveguide supports an even mode and an odd mode [Figs. 2(a) and 2(b)]. The dispersion relation (frequency ω as a function of propagation constant k) of these modes are shown in Fig. 2(c). At a given frequency

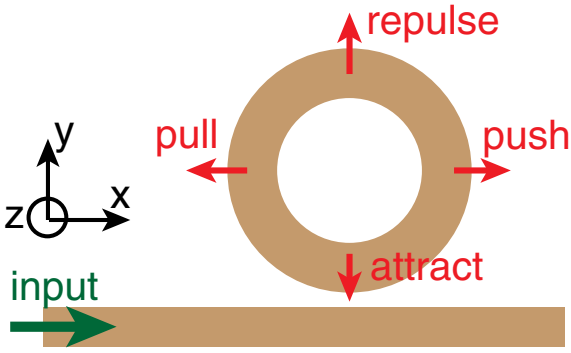

Fig. 1. Schematics of a resonator–waveguide system, with the definition for the force in each direction on the resonator.

ω, the even mode has a higher k, and hence a higher momentum, as compared to the odd mode.

An object placed near the waveguide can scatter light in the waveguide. This may convert an incident photon in one mode into a scattered photon in another mode. If an incident photon is in the high momentum mode, upon scattering into the low momentum mode, the difference in momentum is imparted on the object, giving it a pushing force. On the other hand, if an incident photon is in the low momentum mode, scattering into a high momentum mode gives the object a pulling force. This connection between the modal conversion and the sign of the optical longitudinal force, as shown in Fig. 2(c), can be considered as a waveguide analogue of the free-space pulling force in [5–8].

We support the intuitive picture above regarding the origin of optical pulling force with analytic calculations. Rakich *et al.* [20] show that an optical force F can be calculated as

$$F = -\frac{1}{\omega}\sum_j P_j \frac{\partial}{\partial d}\phi_j, \tag{1}$$

where P_j and ϕ_j are the power and phase of the output at port j, respectively, and d is the relevant displacement. In the configuration of Fig. 1, the j's in Eq. (1) label different waveguide modes that the ring resonator couples to. Note the extra minus sign here in comparison to [20] because we use the $\exp(+i\omega t)$ sign convention. To apply this formula to the waveguide–resonator system, we measure the input at $x = 0$ and the output at $x = L$, and assume that the resonator is located at $x = x_r < L$. Because we are interested in the longitudinal force on the resonator, d in Eq. (1) is taken to be x_r. Let k_{in} be the propagation constant of the input mode, and k_j be the propagation constant of each output mode. Eq. (1) then becomes

$$F = -\frac{1}{\omega}\sum_j P_j \frac{\partial}{\partial x_r}\phi_j, \tag{2}$$

$$\phi_j = -k_{\text{in}}x_r + \theta_j - k_j(L - x_r), \tag{3}$$

where θ_j is the phase shift due to the coupling with the resonator, which is independent of x_r. Note that all the output channels, including both the scattering in the waveguide as well as radiation or material loss, have to be included in Eq. (1). For scattering in the waveguide, we use the appropriate k_j for the corresponding waveguide modes. For scattering into radiation modes, we use the average forward wavevector of the radiation modes. In most cases, including our example of a ring resonator below, the resonator is symmetric in $\pm x$ direction. Therefore, the forward and the backward scattering from these resonators are equal; hence k_j for these scattering modes can be taken to be zero. This conclusion is consistent with our direct numerical calculation of the waveguide–resonator force. Similarly, for material loss, we set $k_j = 0$. From Eqs. (2) and (3), the force is then

$$F = -\frac{1}{\omega}\sum_j P_j(\Delta k)_j, \tag{4}$$

where $(\Delta k)_j = k_j - k_{\text{in}}$. We can also write the input power in terms of photon flux in each output mode (Φ_j) as $P_j = \Phi_j \hbar\omega$, where $\hbar$ is Planck's constant. Therefore, we can write

$$F = -\sum_j \Phi_j \hbar(\Delta k)_j. \tag{5}$$

This means that the longitudinal force per photon comes from the exchange of momentum $\hbar(\Delta k)_j$ as described in the intuitive explanation above.

Motivated by the theoretical considerations above, we next provide a numerical example. We couple the waveguide described above with a ring resonator shown in Figs. 3(a) and 3(b). Even though any object that can create mode mixing in a waveguide can experience an optical pulling force, we use a resonator structure that can achieve efficient mode mixing in order to achieve a large pulling force. We use a silicon ring resonator with an outer radius of $4.3a$, inner radius of $3.9a$, and permittivity of 12.1. The silicon region is sufficiently narrow that a waveguide with the same silicon width supports only the fundamental mode. The gap between the resonator and the waveguide is $0.1a$.

In Figs. 3(c) and 3(d), we plot the output power in each mode per input power (P_j/P_{in}) as a function of frequency when we excite either the even or odd modes in the waveguide. We see that the two waveguide modes excite the same set of resonances. At the incident wave frequency $\omega = 0.65 \times 2\pi c/a$, where c is the speed of light in vacuum, we show the steady-state field distribution, in Figs. 3(a) and 3(b), when we excite either the even

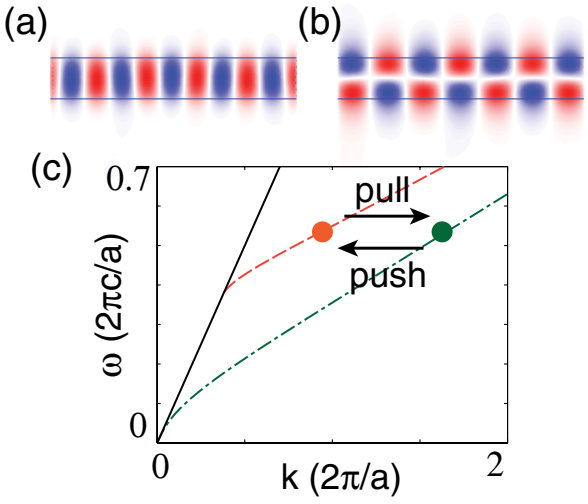

Fig. 2. Modal field pattern of a waveguide with width $0.4a$, permittivity of 12.1, at $\omega = 0.65 \times 2\pi c/a$, in (a) the even mode and (b) the odd mode. The red (dark grey) and blue (light grey) represents positive and negative electric fields in the z direction. (c) Dispersion relation of the above waveguide for the even mode (dashed–dotted line) and the odd mode (dashed line). The solid line is the light line $\omega = ck$.

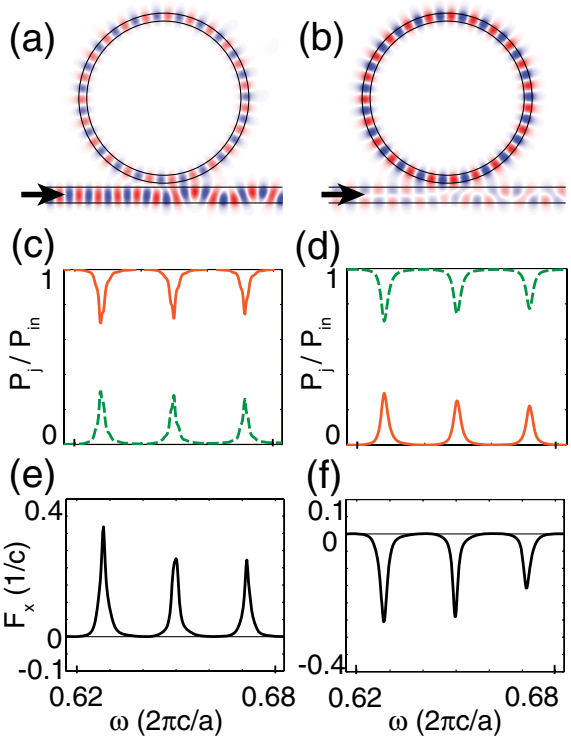

Fig. 3. Field pattern of the resonator–waveguide system. The resonator has permittivity of 12.1, outer radius of $4.3a$, and inner radius of $3.9a$. The gap between the resonator and waveguide has a width of $0.1a$. The frequency is $\omega = 0.65 \times 2\pi c/a$. The inputs are in the waveguide's (a) even mode and (b) odd mode. The input direction is denoted with a black arrow. (c) Output power in each mode per input power (P_j/P_{in}) when the input is in the even mode. Solid lines denote the even mode output, dashed lines denote the odd mode output. (d) Same as (c) but with the input in the odd mode. F_x per input power as a function of ω for the input in the waveguide's (e) even mode and (f) odd mode.

mode or the odd mode in the waveguide. As can be seen in Figs. 3(c) and 3(d), we observe significant modal conversion when the input consists of either mode. As shown in Figs. 3(e) and 3(f), due to the mode conversion, the resonator experiences a pushing force if the input is in the waveguide's even mode and a pulling force if the input is in the waveguide's odd mode, in consistency with the theory above. By inducing strong modal conversion, the resonance is responsible for achieving a large longitudinal pulling or pushing force.

In this example, the input in both modes can couple with the resonator due to the approximate phase matching between the traveling wave in the ring and that in the waveguide. Specifically, at this frequency, the even and odd modes of the waveguide have the propagation constant k of $2.07 \times 2\pi/a$ and $1.43 \times 2\pi/a$, respectively, while the $0.2a$ wide waveguide that makes up the ring resonator has $k = 1.78 \times 2\pi/a$. In our case, because of the small radius of the curvature of the ring, the coupling between the waveguide and the ring does not require exact phase matching, and our numerical results here indicate that the phase mismatch is sufficiently small that both input modes couple to the same resonator mode of the ring, resulting in large modal conversion. In this system, the odd mode is closer to critical coupling, and hence has a higher energy in the resonator, as can been seen by comparing Figs. 3(a) and 3(b). Also, note that the resonator–waveguide gap is small, such that the coupling between the resonator and the waveguide in either mode is much larger than the radiation loss; hence, very little power is lost into the radiation mode. This can be seen from Figs. 3(c) and 3(d), where the sum of the power fraction of the two output modes is very close to 1.

To demonstrate the pulling force, one can consider a configuration similar to what was shown in [21,22], where the suspended ring resonator is connected to a support at its center with thin spokes. With an appropriate dimension and position of the spokes, such as two thin spokes along the y direction, the system should be sensitive enough to the longitudinal optical force that a mechanical response, such as a displacement, can be measured. Another possibility is by using a microfluidics system. For example, Schmidt *et al.* [23] fabricate an optical waveguide under a fluidics channel. A particle in the fluid near the waveguide experiences an optical pushing force. This system may be adapted by using a multimode waveguide with an appropriate optical mode to demonstrate the optical pulling force proposed by our Letter.

As one application of the optical pulling force, we show that such a force can be combined with the optical equilibrium effect discussed in [16] to create an all-optical conveyor belt. Optical stable equilibrium in the waveguide–resonator system means that there exists a gap width d_e between the resonator and the waveguide, such that the lateral optical force is zero if the system is at $d = d_e$, repulsive at $d < d_e$, and attractive at $d > d_e$. Therefore, a resonator under optical stable equilibrium is maintained at the distance d_e by the optical force. By combining the pulling force with the optical stable equilibrium, we can create an all-optical conveyor belt effect, where the resonator does not drift laterally while being pulled along the waveguide. Intaraprasonk and Fan [16] show that optical equilibrium in a resonator–waveguide system can be achieved at frequencies between a pair of overlapping resonances. Because the pulling force occurs from the multimode nature of the waveguide, and the optical equilibrium occurs from the multimode nature of the resonator, these two effects are independent in origin and hence can occur simultaneously.

To illustrate this, we use the same ring resonator except that the inner radius is reduced to $3.3a$. This allows the resonator to support two sets of modes with different transverse modal profiles shown in Figs. 4(a) and 4(b), as is required for an optical equilibrium. In Fig. 4(c), we plot U as a function of ω when we excite the odd mode in the waveguide. Near the frequency $\omega = 0.654 \times 2\pi c/a$, the two sets of resonances overlap, with the second-order resonance at higher frequency. It is then possible to find an optical equilibrium between these two resonances; this is shown in Fig. 4(d), where we plot the lateral force (F_y) on the resonator at $\omega = 0.6552 \times 2\pi c/a$ as a function of the gap between the resonator and the waveguide (d). The lateral force is repulsive for $d < 0.096a$ and attractive for $d > 0.096a$, creating a lateral optical equilibrium at $d = 0.096a$. The longitudinal force on the resonator plotted in the same figure shows the pulling force on

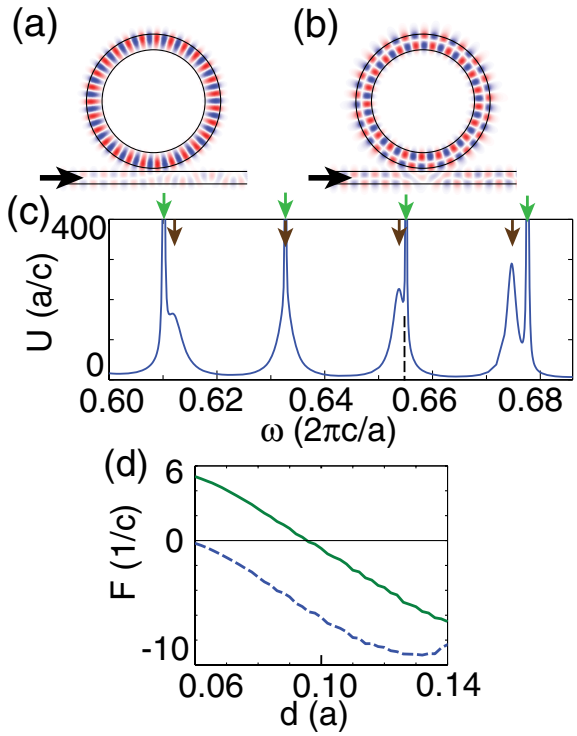

Fig. 4. Field pattern of the resonator–waveguide system with the same parameters as Fig. 3, except that the ring has the inner radius of $3.3a$ instead. The input is in the waveguide's odd mode. (a) First-order resonance at $\omega = 0.6776 \times 2\pi c/a$. (b) Second-order resonance at $\omega = 0.6747 \times 2\pi c/a$. The input direction is denoted with a black arrow. (c) U as a function of ω for the input in the waveguide's odd mode. Light green arrows denote the first-order resonances, dark brown arrows denote the second-order resonances. (d) $F_x \times 10$ (dotted line) and F_y (solid line) per input power of the system at $\omega = 0.6552 \times 2\pi c/a$.

the resonator. This illustrates the conveyor belt effect, where the lateral optical force keeps the resonator at a constant distance from the waveguide while the pulling force pulls the resonator toward the light source. Note that this conveyor belt effect can also be achieved with an optical pushing force in this same structure by simply exciting the even mode in the waveguide at an appropriate frequency.

This work is supported by an AFOSR-MURI program on Integrated Hybrid Nanophotonic Circuits (Grant No. FA9550-12-1-0024). S. F. acknowledges discussions with Prof. Michal Lipson.

References

1. A. Dogariu, S. Sukhov, and J. J. Saenz, Nat. Photonics **7**, 24 (2012).
2. S. M. Block, Nature **360**, 493 (1992).
3. T. Cizmar, V. Kollarova, Z. Bouchal, and P. Zemanek, New J. Phys. **8**, 43 (2006).
4. D. B. Ruffner and D. G. Grier, Phys. Rev. Lett. **109**, 163903 (2012).
5. O. Brzobohaty, V. Karasek, M. Siler, L. Chvatal, T. Cizmar, and P. Zemanek, Nat. Photonics **7**, 123 (2013).
6. J. Chen, J. Ng, Z. Lin, and C. T. Chan, Nat. Photonics **5**, 531 (2011).
7. A. Novitsky, C. Qiu, and H. Wang, Phys. Rev. Lett. **107**, 203601 (2011).
8. S. Sukhov and A. Dogariu, Phys. Rev. Lett. **107**, 203602 (2011).
9. A. Ashkin and J. M. Dziedzic, Phys. Rev. Lett. **38**, 1351 (1977).
10. Y. Li, O. V. Svitelskiy, A. V. Maslov, D. Carnegie, E. Rafailov, and V. N. Astratov, Light: Sci. Appl. **2**, e64 (2013).
11. D. Van Thourhout and J. Roels, Nat. Photonics **4**, 211 (2010).
12. A. Einat and U. Levy, Opt. Express **19**, 20405 (2011).
13. V. Intaraprasonk and S. Fan, Phys. Rev. A **86**, 063833 (2012).
14. M. Eichenfield, C. P. Michael, R. Perahia, and O. Painter, Nat. Photonics **1**, 416 (2007).
15. M. Li, W. H. P. Pernice, and H. X. Tang, Phys. Rev. Lett. **103**, 223901 (2009).
16. V. Intaraprasonk and S. Fan, http://arxiv.org/abs/1306.2417.
17. J. J. Xiao, J. Ng, Z. F. Lin, and C. T. Chan, Appl. Phys. Lett. **94**, 011102 (2009).
18. J. J. Xiao, H. H. Zheng, Y. X. Sun, and Y. Yao, Opt. Lett. **35**, 962 (2010).
19. "Comsol Multiphysics," www.comsol.com.
20. P. T. Rakich, M. A. Popovic, and Z. Wang, Opt. Express **17**, 18116 (2009).
21. G. S. Wiederhecker, L. Chen, A. Gondarenk, and M. Lipson, Nature **462**, 633 (2009).
22. G. S. Wiederhecker, S. Manipatruni, S. Lee, and M. Lipson, Opt. Express **19**, 2782 (2011).
23. B. S. Schmidt, A. H. J. Yang, D. Erickson, and M. Lipson, Opt. Express **15**, 14322 (2007).